

The Oxidant Thimerosal Modulates Gating Behavior of KCNQ1 by Interaction with the Channel Outer Shell

G. Kerst¹, H. Brouzos², R. Schreiber³, R. Nitschke², M.J. Hug⁴, R. Greger², M. Bleich⁵

¹University Children's Hospital, Hoppe-Seyler-Strasse 1, 72076 Tübingen, Germany

²Physiologisches Institut der Albert-Ludwigs-Universität Freiburg, Hermann-Herder-Straße 7, 79104 Freiburg, Germany

³Department of Physiology & Pharmacology, University of Queensland, St. Lucia, QLD 4072, Brisbane, Australia

⁴Physiologisches Institut der Westfälischen Wilhelms-Universität Münster, Robert-Koch-Str. 27a, 48149 Münster, Germany

⁵Aventis Pharma, Bld. H821, D-65926 Frankfurt, Germany

Received: 13 August 2001/Revised: 20 November 2001

Abstract. Thimerosal (*o*-Ethylmercurithio)benzoic acid, TMS), a membrane-impermeable, sulfhydryl-oxidizing agent, has been described to increase the K⁺ current I_{Ks} in KCNE1-injected *Xenopus laevis* oocytes. Since there are no cysteine residues in the extracellular domain of KCNE1, it has been proposed that TMS interacts with its partner protein KCNQ1. The aim of this study was therefore to investigate the interaction of TMS with KCNQ1 and the respective K⁺ current I_K . In CHO cells stably transfected with KCNQ1/KCNE1, TMS increased I_{Ks} , whereas in CHO cells expressing KCNQ1 alone, TMS initially decreased I_K . TMS also affected the cytosolic pH (pH_i) and the cytosolic Ca²⁺ activity ([Ca²⁺]_i) in these cells. TMS slowly decreased pH_i. With a short delay, TMS increased [Ca²⁺]_i by store depletion and capacitative influx. The time course of the effects of TMS on pH_i and [Ca²⁺]_i did not correlate with the effect of TMS on I_K . We therefore anticipated a different mode of action by TMS and investigated the influence of TMS on cysteine residues of KCNQ1. For this purpose, KCNQ1_{wt} and two mutants lacking a cysteine residue in the S6 or the S3 segment (KCNQ1_{C331A} and KCNQ1_{C214A}, respectively) were expressed in *Xenopus laevis* oocytes. A sustained current decrease was observed in KCNQ1_{wt} and KCNQ1_{C331A}, but not in KCNQ1_{C214A}-injected oocytes. The analysis of tail currents, I/V curves and activation kinetics revealed a complex effect of TMS on the gating of KCNQ1_{wt} and KCNQ1_{C331A}. In another series we investigated the effect of TMS on I_{Ks} . TMS increased I_{Ks} of

KCNQ1_{C214A}/KCNE1-injected oocytes significantly less than I_{Ks} in KCNQ1_{wt}/KCNE1- or KCNQ1_{C331A}/KCNE1-injected cells. These results suggest that thimerosal interacts with the cysteine residue C₂₁₄ in the S3 segment of KCNQ1, leading to a change of its gating properties. Our results support the idea that not only the inner shell, but also the outer shell of the channel is important for the gating behavior of voltage dependent K⁺ channels.

Key words: 293B — Oxidant stress — Structure-function relationship — KCNQ1

Introduction

The modification of cysteine residues by redox agents has been useful in establishing structure-function relationships of a variety of ion channels [4, 5, 23, 25]. Depending on the protein and the sulfhydryl reagent, the oxidation of cysteine residues can either lead to disulfide bonds in between the protein (or proteins) or it may result in the attachment of an adduct that is part of the reagent. TMS is a hydrophilic, membrane-impermeable sulfhydryl oxidant and therefore modifies cysteine residues that are located in or close to the extracellular space. The reaction of TMS with the sulfhydryl group results in an attachment of an ethylmercurithio-group. Recently, the effect of TMS on the slow delayed-rectifier current I_{Ks} has been investigated in KCNE1-injected *Xenopus laevis* oocytes [33]. TMS was shown to increase the amplitude, to accelerate activation and to slow deactivation of I_{Ks} . At that time it was unknown that in these cells KCNE1 coassembles with the endogenously

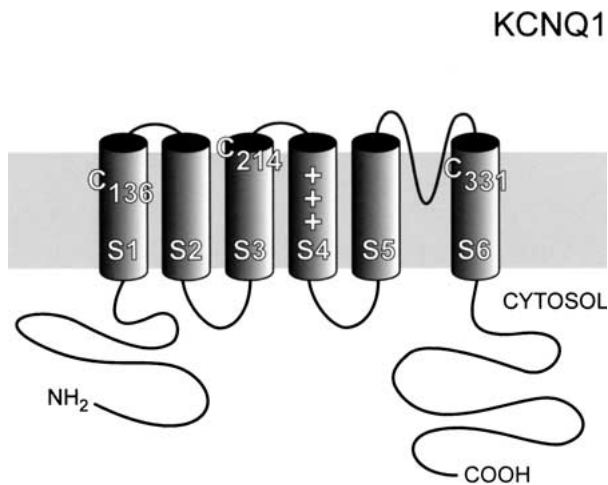


Fig. 1. Membrane topology of KCNQ1 [32]. The positions of the three cysteine residues at position 136, 214 and 331, which are located closely to the extracellular space, are indicated. The three cysteines are conserved in *Xenopus laevis* KCNQ1.

expressed partner protein xKCNQ1 to form heteromeric channels as the molecular basis of I_{Ks} [24]. Since the amino-acid sequence of KCNE1 does not contain a cysteine residue in the extracellular domain it was proposed that TMS interacts with a putative partner protein of KCNE1. In this study we investigated the effect of TMS on homomeric KCNQ1 and heteromeric KCNQ1/KCNE1 channels. The amino-acid sequence of the human KCNQ1 channel displays 3 cysteines located close to the extracellular space at positions 136, 214 and 331 (Fig. 1). We report on the complex effects of TMS on the gating properties of homomeric KCNQ1 channels. The use of cysteine mutants strongly suggests that TMS interacts with the cysteine residue C₂₁₄, which is located in the outer part of the S3 segment. We propose that this channel region is involved in the complex interplay of gating of homomeric KCNQ1 as well as of heteromeric KCNQ1/KCNE1 channels.

Materials and Methods

CELL CULTURE AND STABLE TRANSFECTION OF CHO-K1 CELLS

Experiments were performed in CHO-K1 cells stably transfected with hKCNQ1/hKCNE1 or hKCNQ1 alone. Positive clones were detected using RT-PCR and electrophysiological analysis. The respective plasmids were pcDNA3.1-hKCNQ1 and pcDNA3.1zeo-hKCNE1. The plasmids used for transfection encoded the full-length sequences of hKCNQ1, isoform 1 [32] and human KCNE1, respectively. CHO-K1 cells stably coexpressing hKCNQ1/hKCNE1 as well as the plasmid pcDNA3.1-hKCNQ1 were kindly provided by Dr. H. W. Jansen, Aventis Pharma, Frankfurt, Germany. CHO-K1 cells were cultured and seeded as described [28, 31]. For transfection with the plasmid pcDNA3.1-hKCNQ1, cells were grown in a 60-mm tissue culture dish and incubated with a mixture

of 5 μg cDNA, [2,3-dioleoyloxy]propyl)-*N,N,N*-trimethylammonium methylsulfate (DOTAP) and phosphate buffer solution for 24 h following the recommendations of the distributor (Boehringer Mannheim, Mannheim, Germany). After the incubation period, the incubation mixture was aspirated and replaced by a cell culture medium containing 250 $\mu\text{g}/\text{ml}$ Geneticin (G418, Life Technologies, Karlsruhe, Germany). Cells were grown to subconfluency, trypsinated and seeded as single cells again in 60-mm tissue culture dishes. Clones were picked 5–7 days after seeding. Antibiotic selection (250 $\mu\text{g}/\text{ml}$ Geneticin or 250 $\mu\text{g}/\text{ml}$ Geneticin plus 250 $\mu\text{g}/\text{ml}$ Zeocin (Invitrogen, San Diego, CA) was continued until the day of the experiment.

PATCH-CLAMP RECORDINGS

Patch-clamp recordings were performed in whole-cell mode at 37°C. The seal resistances were ≥ 1 G Ω . The resistances of the patch pipettes were around 4 M Ω when filled with the pipette solution for whole-cell recordings. A flowing (1 mol/l) KCl electrode served as a bath reference. The pipette and the whole-cell capacitance were cancelled using the compensation circuits of the amplifier (U. Fröbe and R. Busche, this institute) with the help of sine wave command voltage [9]. Voltage-clamp protocols were performed as shown in Results. The data were low-pass filtered at 10 kHz and stored on digital audio tape (digitalization rate 32 kHz). The analysis was performed from the online record. The pipette solution for whole-cell recordings was adjusted to pH 7.2 and contained in mM: K-gluconate 95; KCl 30; NaH₂PO₄ 1.2; Na₂HPO₄ 4.8; Ca-gluconate 0.73; MgCl₂ 2.4; 1,2-bis-(2-aminoethoxy)ethane-*N,N,N',N'*, tetraacetic acid (EGTA) 1; D-glucose 5; adenosine 5'-triphosphate (ATP) 3. The pipette solution for the investigation of a $[\text{Ca}^{2+}]_i$ dependence of KCNQ1 currents in CHO cells did not contain Ca-gluconate and the EGTA concentration was increased to 10 mM. The standard bath solution (control) contained in mM: NaCl 145; K₂HPO₄ 1.6; KH₂PO₄ 0.4; Ca-gluconate 1.3; MgCl₂ 1; D-glucose 5. The “low Ca^{2+} ” solution with a Ca^{2+} activity of 10^{-6} M was derived from control with Ca-gluconate 0.96 and EGTA 1. In the acetate-containing solution, 20 mM NaCl were replaced by 20 mM Na-acetate. The pH of all bath solutions was 7.4 and readjusted after the addition of TMS and 2,3-Dihydroxybutane-1,4-dithiol (DTE, Dithioerythritol). All compounds used were of highest available grade of purity and obtained from Sigma (Deisenhofen, Germany) and Merck (Darmstadt, Germany). 293B (trans-6-cyano-4-(*N*-ethylsulfonyl-*N*-methylamino)-3-hydroxy-2,2-dimethylchromane) was a kind gift of Aventis Pharma, Frankfurt, Germany.

FLUORESCENCE MEASUREMENTS OF pH_i AND $[\text{Ca}^{2+}]_i$ IN CHO CELLS

The experiments were performed as described in detail elsewhere [15, 16]. In brief, CHO cells were loaded at room temperature for 40–60 min with BCECF/AM (30 μM) or fura-2/AM (20 μM), respectively and pluronic F127 (80 μM) was added to improve dye loading. During the experiments cells were continuously superfused with control solution at 37°C at a bath solution exchange rate of 1 Hz. The emission signal was collected from an average of 6–8 cells at a time resolution of 10 Hz. BCECF was excited at 436 nm and 488 nm. Emission was recorded between 515 and 565 nm and the 488 nm/436 nm ratio was calculated. The calibration of the ratio signal to pH units was performed by the use of nigericin (40 μM) and high-K⁺ buffer solutions (145 mM) of defined pH (6.5; 7.0; 7.5; 8.0). Fura-2 was excited at 340 nm, 360 nm and 380 nm. The emission was recorded at 500–530 nm and the emission ratio 340 nm/380 nm served as a measure of $[\text{Ca}^{2+}]_i$. Calibration of the ratio

as described in [7, 15] was not successful because no reliable R_{\max} values could be obtained in CHO cells [31]. For comparison, peak ratios induced by the purinergic agonist ATP (0.1 mM) are given as reference signal.

ISOLATION OF *XENOPUS LAEVIS* OOCYTES, MUTAGENESIS, PREPARATION OF cRNA, MICROINJECTION OF cRNA AND DOUBLE VOLTAGE MEASUREMENTS

The oocytes were isolated from adult *Xenopus laevis* female frogs (H. Kähler, Bedarf für Entwicklungsbiologie, Hamburg), dispersed and defolliculated by a 0.5-hr treatment with collagenase (type A, Boehringer, Germany). Afterwards, the oocytes were rinsed and kept at 18°C in an ND96-buffer containing (in mM) NaCl 96, KCl 2, CaCl₂ 1.8, MgCl₂ 1, 1,4-(2-hydroxyethyl)-l-piperazineethanesulphonic acid (HEPES) 5, Na-pyruvate 2.5. The solution was adjusted to pH 7.55 and supplemented with theophylline (0.5 mM) and gentamycin (5 mg/l). Oocytes of identical batches were injected each with 30 ng of the respective copy RNA (cRNA) dissolved in 50 nl double-distilled H₂O by a pneumatic pico pump (PV830, WPI, Germany). Oocytes serving as controls were injected with 50 nl double-distilled H₂O only. For cRNA synthesis, the plasmid pSP64-hKCNQ1 (kindly provided by M. Keating and M. Sanguinetti, University of Utah, UT) was linearized with EcoRI and transcribed in vitro using Sp6 polymerase and a 5' cap (mCAP mRNA capping kit, Stratagene, La Jolla, CA). *NotI*, T7 polymerase and a 5' cap were used for linearization and in vitro transcription of pBS-hKCNE1 (kindly provided by A. E. Busch, Aventis, Frankfurt, Germany).

Mutations of hKCNQ1 were generated by polymerase chain reaction using the QuikChange site-directed mutagenesis kit according to the manufacturer's instructions (Stratagene). The following sense (*s*) and antisense (*as*) oligonucleotides were used: KCNQ1_{C214A}, (*s*) 5'-GGTGGTCTCGCCGTGGGATCCAAGGGGC-3' (*as*) 5'-GCCCTTGGATCCCACGGCGAGGACCA-3'; KCNQ1_{C331A}, (*s*) 5'-GGAAGACCATCGCTAGCG CCTCTCTGTC-3', (*as*) 5'-GACAGAGAAGGCGCTAGCGATGGTCTTCC-3'. The mutations were confirmed by cycle sequencing (PRISM, Perkin-Elmer).

Oocytes were impaled 2–4 days after cRNA injection with two electrodes (Clark, UK), which had resistances of ≤ 1 M Ω when filled with 2.7 mol/l KCl. A flowing (2.7 mol/l) KCl electrode served as a bath reference. Membrane currents were recorded by voltage clamping of oocytes (OOC-1, WPI, Germany) as mentioned in the Results. Currents were filtered at 200 Hz. The data were collected continuously at a 1000 Hz sample frequency on a computer hard disc and analyzed using the programs' chart and scope (McLab, AD-Instruments, Macintosh). The experiments were performed at room temperature. The bath solution contained (in mM): Na-gluconate 96; KCl 2; Ca-gluconate 5; MgCl₂ 1; HEPES 5; Na-pyruvate 2.5. The pH of the solution was adjusted to 7.55 by NaOH and readjusted after the addition of TMS and DTE prior to use.

DATA ANALYSIS

The data are shown as individual measurements and mean values \pm SEM with n as the number of observations. The paired and unpaired Student's *t*-tests were used to test for statistical significance ($P < 0.05$). All the data in the result section refer to total currents. The only exception was the analysis of currents in the right panels of Fig. 2, in which values after subtraction of the nonspecific baseline current are shown [31]. Time dependence of the currents

was determined using a Levenberg-Marquardt algorithm (Origin 5.0, Microcal Software, Inc., Northampton, MA). Activation kinetics were fitted with the function

$$I_0 + I_1 e^{(-t/\tau_1)} + I_2 e^{(-t/\tau_2)} \quad (1)$$

deactivation kinetics with the function

$$I_0 + I_1 e^{(-t/\tau)} \quad (2)$$

Results

EFFECT OF TMS ON I_{Ks} AND I_K CURRENTS IN TRANSFECTED CHO CELLS

Figure 2A depicts the effect of 0.1 mM TMS on KCNQ1/KCNE1 currents (I_{Ks}) in stably transfected CHO cells. TMS induced an instantaneous increase of I_{Ks} current by $153 \pm 56\%$ of its control value ($n = 7$). This current increase has been described for I_{Ks} in KCNE1-injected *X. laevis* oocytes [33]. In agreement with this report on I_{Ks} in oocytes, the current increase in CHO cells was not reversible after washout of TMS (*not shown*). The effect of TMS on KCNQ1 currents (I_K) in CHO cells was more complex, as demonstrated in Fig. 2B. After an instantaneous reduction in current by $20 \pm 7\%$ ($n = 9$), a delayed increase in current by $67 \pm 24\%$ could be observed ($n = 10$). To observe the current increase, cells had to be superfused on average for approximately 1 min with TMS. Our experience was that a stable whole-cell recording was very difficult to maintain while TMS was present in the bath solution. Therefore, the effect of withdrawal of TMS could only be observed in 3 experiments. In contrast to the persistent effect of TMS on I_{Ks} , the augmentation of I_K was reversible after washout of TMS in these experiments (*not shown*). This observation and the biphasic effect of TMS on I_K pointed to a more complex effect of TMS on KCNQ1 than just a simple oxidation of cysteine residues. Since I_{Ks} as well as I_K currents are affected by $[Ca^{2+}]_i$ and pH_i [3, 31] and since the effect of TMS on $[Ca^{2+}]_i$ and pH_i has not been investigated so far in CHO cells, we examined the effect of TMS on these parameters.

EFFECT OF TMS ON pH_i AND $[Ca^{2+}]_i$ IN CHO CELLS

The addition of 0.1 mM TMS decreased cytosolic pH significantly by 0.34 ± 0.07 pH units ($n = 6$, Fig. 3A, lower panel). This acidification started immediately after the addition of TMS to the bath and slowly increased over time (Fig. 3A, upper panel). Washout of TMS did not lead to a pH_i change. A recovery of pH_i to baseline values was only observed after the addition of 5 mM DTE (alkalinization by 0.45 ± 0.1 pH units). For comparison, a solution

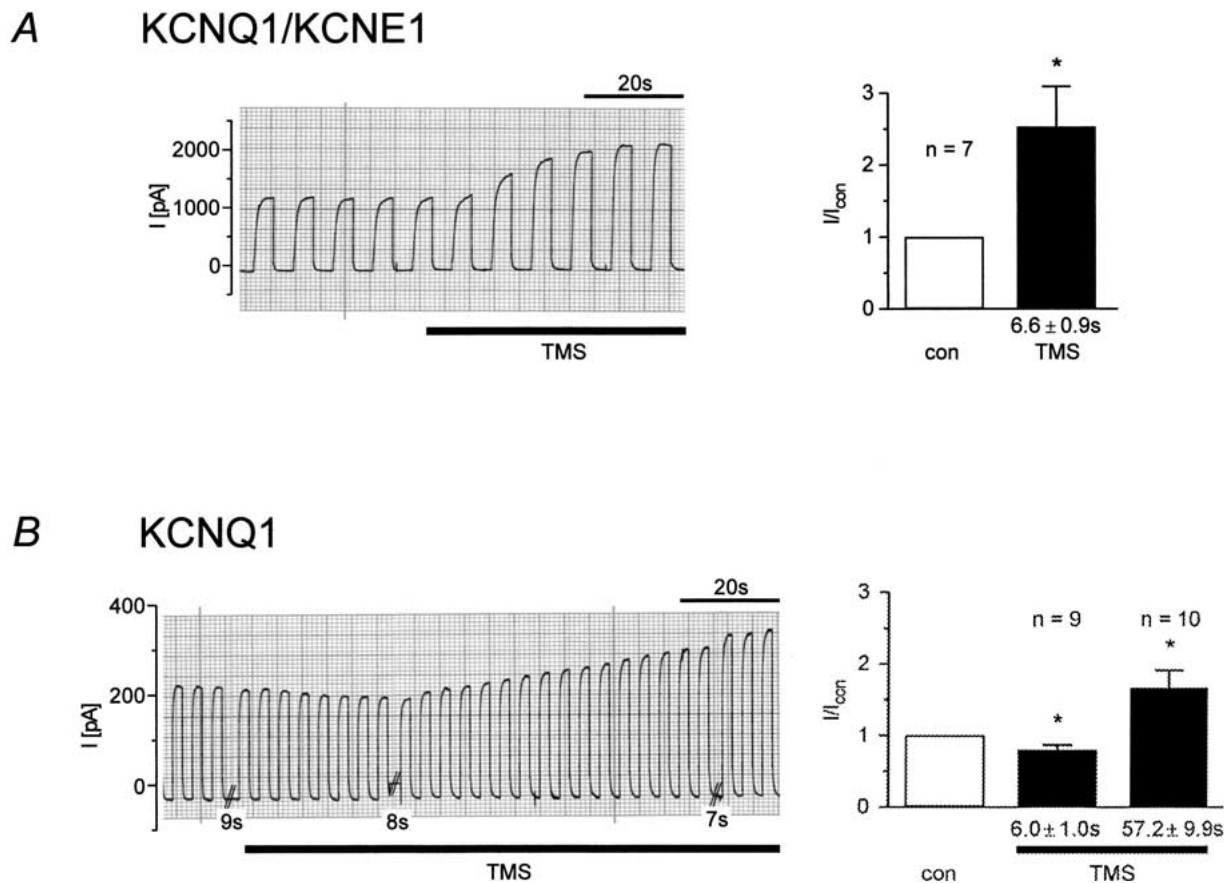


Fig. 2. Effect of 0.1 mM thimerosal (TMS) on KCNQ1/KCNE1 (I_{Ks}) and KCNQ1 (I_K) currents in CHO cells (*left panels*: original recordings, *right panels*: series of experiments). (*A*) TMS increased I_{Ks} immediately, i.e., 6.6 ± 0.9 sec after the addition of TMS the beginning of the current increase could be detected. (*B*) I_K showed an initial inhibition and a delayed increase by 0.1 mM TMS. The beginning of the current decrease and increase could be detected after 6.0 ± 1.0 sec ($n = 8$) and 57.2 ± 9.9 sec ($n = 9$) after the

addition of TMS, respectively. The time delay and the size of the initial reduction in current could not be estimated in all 10 experiments, since in the respective experiments the cells were held at their membrane voltages at the relevant time. In the original recording, the measurement was interrupted three times to measure input conductance and membrane capacitance. I_{Ks} - and I_K -currents were elicited by 4-sec and 2-sec voltage clamp pulses from -60 to 0 mV, respectively.

containing 20 mM acetate was given in these experiments in a paired fashion. The addition of acetate led to an acidification by 0.58 ± 0.06 , the withdrawal to a realkalinization by 0.59 ± 0.06 pH units. In a previous study we showed that the acidification by 20 mM acetate decreased I_K by some 20%, while it increased I_{Ks} by about 60% [31]. In spite of this finding, the acidification by TMS is probably not the key signal for the initial effects seen on I_K and I_{Ks} after the addition of TMS. While the effect of TMS on the currents could be observed immediately after the addition of the sulfhydryl-reagent to the bath, the acidification increased slowly in a linear fashion over some 3 min during the presence of TMS in the bath (Fig. 3A, upper panel).

It has been shown previously that I_K is activated by a rise in $[Ca^{2+}]_i$ [31]. Therefore, we investigated the effect of TMS on $[Ca^{2+}]_i$ in fura-2-loaded CHO cells. The original recording shown in Fig. 3B represents one of 5 very similar experiments. In these ex-

periments, 0.1 mM TMS increased $[Ca^{2+}]_i$ in a bath solution containing 10^{-6} M Ca^{2+} ("low Ca^{2+} ") as well as in the presence of a control solution containing 1.3 mM Ca^{2+} ("con"). Under both conditions the Ca^{2+} increase occurred with a delay of some 30 sec, which could indeed coincide with the increase of I_K . Yet, while the withdrawal of TMS reversed the increase of I_K it did not reverse the rise in $[Ca^{2+}]_i$. After the washout of TMS and in the presence of external Ca^{2+} , $[Ca^{2+}]_i$ remained high and returned to baseline values only after the addition of 5 mM DTE. Since absolute values for $[Ca^{2+}]_i$ could not be obtained in CHO cells [31], 0.1 mM ATP was given in each experiment in order to estimate the magnitude of the TMS-induced rise in $[Ca^{2+}]_i$. ATP and TMS caused a comparable increase in $[Ca^{2+}]_i$. In 8 paired experiments, in which the addition of ATP and TMS was permuted. ATP increased the fluorescence ratio 340 nm/380 nm by 1.4 ± 0.1 and TMS by 1.2 ± 0.1 units (peak values), respectively.

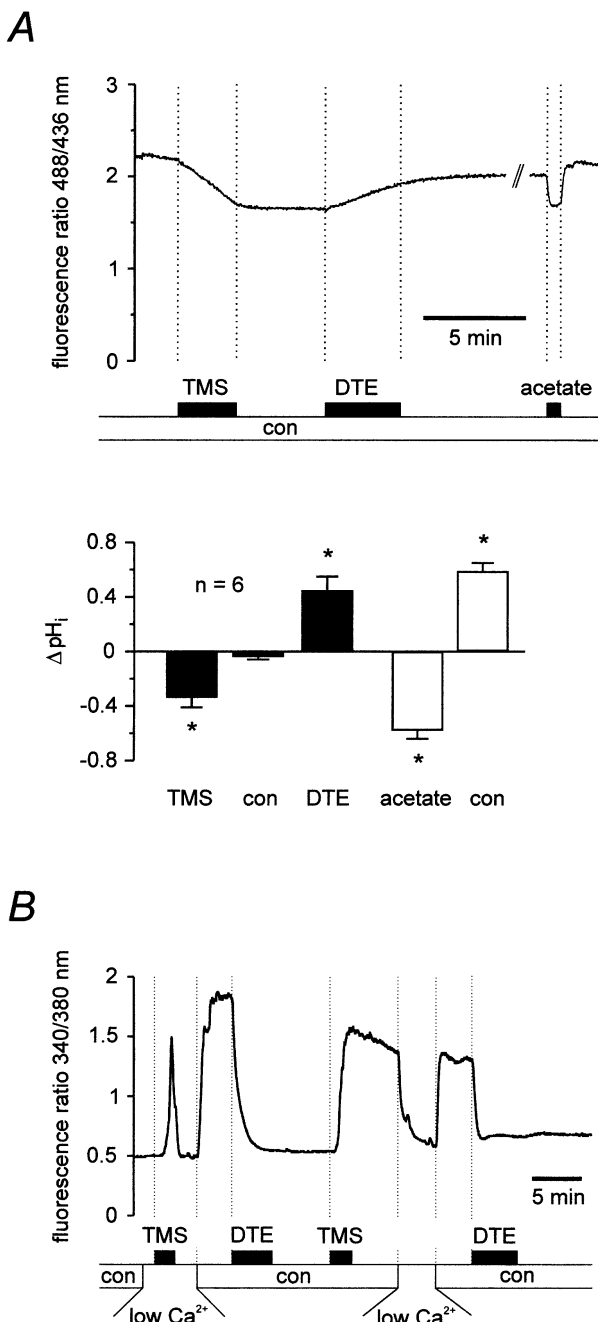


Fig. 3. Effect of TMS and dithioerythritol (DTE), a sulfhydryl-reducing reagent, on cytosolic pH (pH_i) and Ca^{2+} ($[\text{Ca}^{2+}]_i$). (A) (upper panel: original recording, lower panel: series of experiments) 0.1 mM TMS acidified pH_i . This acidification was not reversed by the washout ("con") of TMS, but by the addition of 5 mM DTE. The reversible acidification of pH_i by 20 mM acetate in the bath is shown for comparison. (B) TMS increased $[\text{Ca}^{2+}]_i$ in bath solutions containing 10^{-6} M Ca^{2+} ("low Ca^{2+} ") and 1.3 mM Ca^{2+} ("con") with a delay of some 30 sec. Again, the effect was not reversible by washout of TMS but by 5 mM DTE.

We also performed patch-clamp recordings in the fast whole-cell mode with a pipette solution containing 10 mM EGTA and a bath solution containing 10^{-6} M Ca^{2+} . Under these conditions we assumed

$[\text{Ca}^{2+}]_i$ to be clamped. Nevertheless, 0.1 mM TMS still increased I_K currents by $53 \pm 24\%$ ($n = 7$).

EFFECT OF TMS ON CURRENTS OF KCNQ1_{wt}, KCNQ1_{C331A} AND KCNQ1_{C214A} CHANNELS IN *XENOPUS LAEVIS* OOCYTES

Since TMS-induced changes in pH_i and $[\text{Ca}^{2+}]_i$ did not sufficiently explain the observed effects on I_K and I_{Ks} currents, we directly addressed the question whether these effects are due to an oxidation of cysteines located closely to the extracellular space. For this purpose we expressed KCNQ1_{wt} and two mutants, KCNQ1_{C331A} and KCNQ1_{C214A} in *X. laevis* oocytes. The two mutants did not exhibit altered current characteristics. In a first series, we investigated the effect of 0.1 mM TMS on I_K in this expression system (Fig. 4). The membrane voltage was clamped at -80 mV for 2 sec, at 0 mV for 5 sec and at -60 mV for 5 sec. As shown in Fig. 4A-C (upper panels), TMS decreased currents of KCNQ1_{wt} (I_{Kwt}) and KCNQ1_{C331A} channels (I_{KC331A}) by -177 ± 43 nA ($n = 4$) and -83 ± 20 nA ($n = 4$), respectively. No significant (n.s.) effect was observed on I_{KC214A} (-12 ± 8 nA, n.s., $n = 5$). To investigate if TMS leads to a delayed current increase, the oocytes were superfused for 12–15 min with TMS. No increase in I_{Kwt} , I_{KC331A} , and I_{KC214A} was observed, indicating that this phenomenon depends on the expression system and not on an oxidation of cysteines of KCNQ1. A prolonged washout period of TMS revealed a poor reversibility of the current decrease in KCNQ1_{wt} ($+123 \pm 42$ nA, n.s., $n = 4$) and I_{KC331A} ($+61 \pm 17$ nA, $p < 0.05$, $n = 4$) injected oocytes. The addition of 2.5 mM DTE led to a complete recovery in the size of I_{Kwt} ($+135 \pm 33$ nA, $p < 0.05$, $n = 4$) and I_{KC331A} , ($+52 \pm 10$ nA, $p < 0.05$, $n = 4$). These observations indicate that TMS oxidizes sulfhydryl groups, which is completely reversible only after the addition of a sulfhydryl-reducing substance. No changes in current size were observed in I_{KC214A} , providing strong evidence that a cysteine residue of the S3 region at position 214 is responsible for the effect of TMS on KCNQ1.

Fig. 4A-C (lower panels) shows the effect of TMS on averaged tail currents at -60 mV. It is evident that TMS slowed down the deactivation process of I_{Kwt} and I_{KC331A} but not of I_{KC214A} . The deactivation time constant τ increased from 1.2 ± 0.2 sec under control conditions to 2.9 ± 0.4 sec in the presence of TMS ($n = 6$) and from 1.2 ± 0.1 sec to 2.2 ± 0.2 sec ($n = 4$) for I_{Kwt} and I_{KC331A} , respectively. Deactivation τ of I_{KC214A} was not altered. These effects are again consistent with an oxidation of C₂₁₄ by TMS.

To investigate the effect of TMS on KCNQ1 channels in more detail, we applied 10-sec depolar-

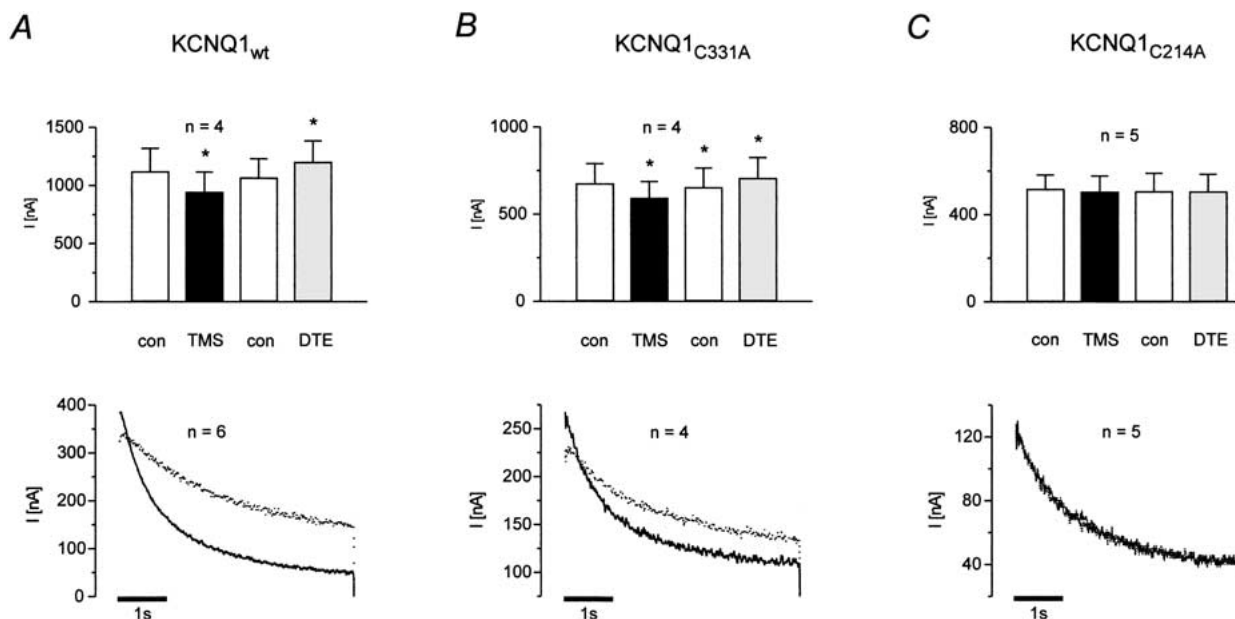


Fig. 4. Effect of 0.1 mM TMS and 2.5 mM DTE on currents of KCNQ1_{wt}, KCNQ1_{C331A} and KCNQ1_{C214A}-injected *X. laevis* oocytes. (A–C) *Upper panels.* In KCNQ1_{wt}- and KCNQ1_{C331A}-injected oocytes, TMS led to a significant inhibition of current at a test voltage of 0 mV. A prolonged washout of TMS (>12 min) led to partial, DTE led to complete recovery of current size. The current of KCNQ_{C214A} was not affected by TMS or DTE. (The

membrane voltage was clamped at -80 mV for 2 sec, at 0 mV for 5 sec and at -60 mV for 5 sec) (A–C) *Lower panels.* Tail currents at -60 mV under control conditions (solid line) and in the presence of 0.1 mM TMS (dotted line). TMS slowed down the deactivation of KCNQ1_{wt} and KCNQ1_{C331A} channels but not of KCNQ1_{C214A} channels. (Same voltage protocol as in A–C, *upper panels*).

izing voltage pulses to membrane potentials of -60 , -40 , -20 and 0 mV from a holding potential of -80 mV. Fig. 5 depicts the corresponding voltage ramps and shows three major findings. First, TMS had again an effect only on I_{Kwt} and I_{KC331A} but not on I_{KC214A} . Second, TMS decreased I_{Kwt} and I_{KC331A} at 0 mV, but increased these currents at -40 mV. Third, TMS changed the activation kinetics of I_{Kwt} and I_{KC331A} .

Fig. 6 shows an analysis of the voltage-dependent effect of TMS in a series of experiments using the same voltage protocol. An evaluation of the current size at the end of the 10-sec depolarizing voltage pulses revealed a complex change in the I/V curve in the presence of TMS for I_{Kwt} and I_{KC331A} , but not for I_{KC214A} (Fig. 6A–C, *upper panels*). This complex change in the I/V relationship by TMS could be confirmed by an analysis of tail currents (*not shown*). An analysis of the current size after 0.2 sec of a depolarizing pulse results in different I/V curves, as shown in Fig. 6A–C, *lower panels*. During this early phase of current activation, TMS enhanced I_{Kwt} and I_{KC331A} at higher depolarizing pulses, while it did not affect I_{KC214A} . When the effect of the KCNQ1-channel blocker 293B on I_K , I_{KC331A} and I_{KC214A} was investigated in the presence of TMS, no difference in inhibition could be detected, neither at a clamp voltage of -40 mV, nor at 0 mV. 30 μ M 293B decreased I_{Kwt} to $50 \pm 4\%$ at -40 mV and to $48 \pm 2\%$ at 0 mV ($n = 6$) and decreased I_{KC331A} and I_{KC214A}

to $49 \pm 6\%$ ($n = 5$) and $46 \pm 3\%$ ($n = 6$) at -40 mV, respectively, and to $48 \pm 4\%$ ($n = 5$) and $46 \pm 2\%$ ($n = 6$) at 0 mV. This observation is consistent with the interpretation that TMS oxidizes the cysteine residue in the S3 region while it leaves the site of the blocker-sensitivity unchanged.

The complex effect of TMS on the activation kinetics was analyzed in more detail in Fig. 7 and Table 1. At -40 mV (Fig. 7, *upper panels*) TMS increased I_{Kwt} and I_{KC331A} throughout the depolarizing step. This current enhancement was accompanied by increasing activation-time constants τ_1 and τ_2 as shown in Table 1. The activation-time constants of I_{KC214A} were not altered. At 0 mV (Fig. 7, *lower panels*) TMS increased I_{Kwt} and I_{KC331A} during the initial phase of activation and decreased these currents during the later phases. The activation-time constants τ_1 and τ_2 of these currents were decreased by TMS, whereas no change of I_{KC214A} could be detected at this voltage. These results clearly indicate that TMS acts via an oxidation of the cysteine residue at position 214 of S3.

Our first experiments provided evidence that the effect of TMS on homomeric KCNQ1 channels might be substantially different from the effect on heteromeric KCNQ1/KCNE1 channels. To investigate the effect of TMS on heteromeric channels, we expressed the following proteins in *X. laevis* oocytes: 1) KCNE1 alone, 2) KCNQ1_{wt} and KCNE1, 3) KCNQ1_{C331A} and KCNE1 and 4) KCNQ1_{C214A} and KCNE1. The

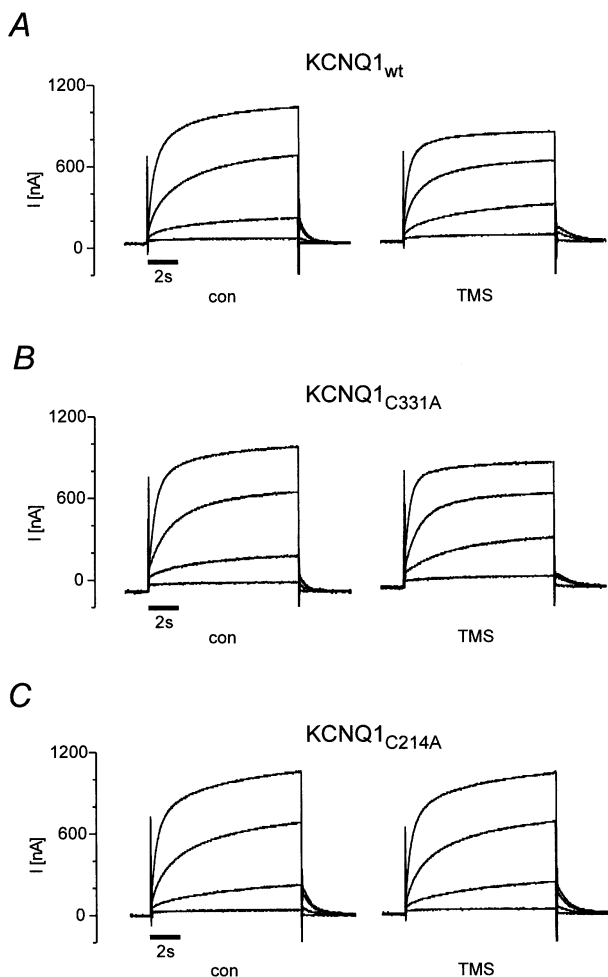


Fig. 5. Effect of TMS on KCNQ1_{wt}, KCNQ1_{C331A} and KCNQ1_{C214A} currents recorded during 10-sec depolarizing pulses to membrane potentials of -60 , -40 , -20 and 0 mV from a holding potential of -80 mV. Note that in KCNQ1_{wt}, KCNQ1_{C331A}-injected oocytes the activation kinetics changed and the current size at -40 mV increased, while it decreased at 0 mV in the presence of TMS.

upper panel of Fig. 8A–D depicts the characteristic sigmoidal slope of current activation of the various heteromeric channels under control conditions and in the presence of 0.1 mM TMS. Oocytes that were injected with KCNE1-cRNA alone exhibited this characteristic slope of current activation upon depolarization as well, which results from heteromerization with endogenous xKCNQ1 subunits. As has been described in the previous report [33], TMS shortened the delay in activation and enhanced the activating currents. The I/V curves of the various heteromeric channels under control conditions and in the presence of 0.1 mM TMS are shown in the lower panels of Fig. 8A–D. As indicated by the asterisks, TMS augmented the different currents at -20 , 0 and $+20$ mV significantly. At first sight it might be surprising that TMS augmented the current of

KCNQ1_{C214A}/KCNE1 channels. It is important to note that the current of xKCNQ1/KCNE1 was increased as well. It seems reasonable to assume that in KCNQ1_{C214A}/KCNE1-injected oocytes, KCNE1 does not only coassemble with KCNQ1_{C214A} but also with endogenous xKCNQ1 subunits. In line with this explanation is the analysis of the current increments at 0 mV by an unpaired Student's t -test. The current increments of KCNE1- and KCNQ1_{C214A}/KCNE1-injected oocytes did not differ from each other, but were different from the current increments of KCNQ1_{wt}/KCNE1- and KCNQ1_{C331A}/KCNE1-injected oocytes. Current increments of KCNQ1_{wt}/KCNE1- and KCNQ1_{C331A}/KCNE1 injected oocytes were not different either. The statistical analysis of current increments suggests that the cysteine residue C₂₁₄ is not only the target of TMS in homomeric KCNQ1 but also in heteromeric KCNQ1/KCNE1 channels.

Discussion

Prompted by a previous study reporting the effect of TMS on I_{Ks} current in *X. laevis* oocytes [33], we investigated whether and how TMS interacts with homomeric KCNQ1 channels.

The first observation to note is that TMS affected currents of homomeric KCNQ1 channels in a different way than currents of heteromeric KCNQ1/KCNE1 channels. In the first set of experiments TMS initially increased I_{Ks} , while it decreased I_K in CHO cells at a clamp voltage of 0 mV. This divergent response underscores once more the well established distinct properties of homomeric and heteromeric channels [2, 31]. Yet, at the time of these experiments it was not clear if TMS exerted this divergent response by a direct effect on cysteine residues of KCNQ1 or via a second messenger induced by the oxidation of sulfhydryl groups of another membrane protein. In fact, TMS has been reported to influence pH_i and $[Ca^{2+}]_i$ [8, 14, 22], second messengers that are known to regulate I_{Ks} and I_K [31]. We have reported recently that cytosolic acidification increases I_{Ks} and decreases I_K [31].

These results prompted us to investigate the effect of TMS on pH_i and $[Ca^{2+}]_i$ in CHO cells. TMS led to a slow and irreversible decrease in pH_i . In spite of the instantaneous onset of the pH_i decrease this second messenger was not likely to explain the divergent responses of I_{Ks} and I_K since pH_i decreased very gradually over some three minutes in a linear manner, while the effect of TMS on I_{Ks} and I_K was maximal after some 30 sec. Next we investigated if TMS affects $[Ca^{2+}]_i$ since an increase in $[Ca^{2+}]_i$ enhances both, I_{Ks} and I_K [31]. Either the initial I_{Ks} or the delayed I_K increase could possibly be explained by a rise in $[Ca^{2+}]_i$. TMS led to a delayed and irre-

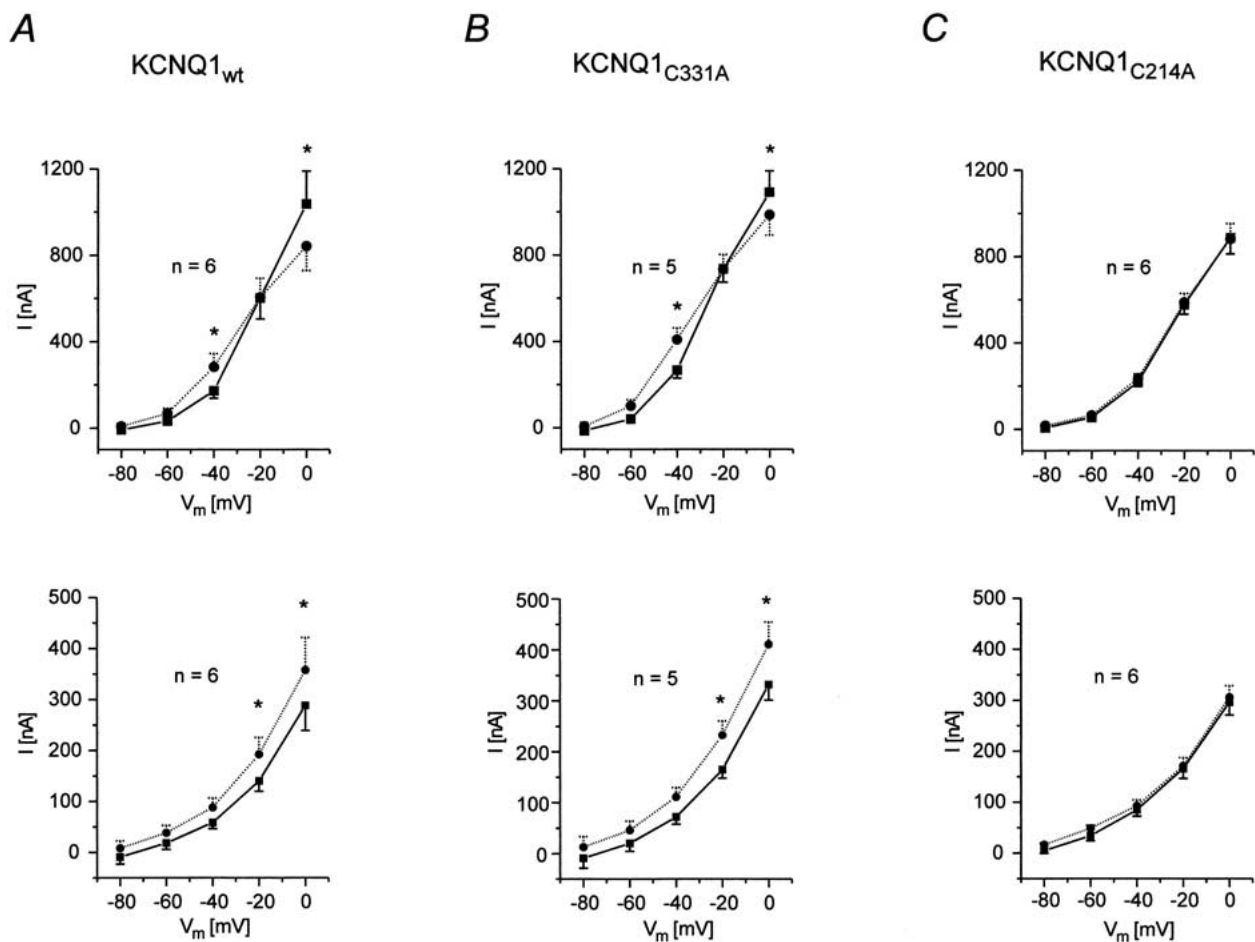


Fig. 6. Effect of TMS on current/voltage (I/V) relationship of $KCNQ1_{wt}$, $KCNQ1_{C331A}$ and $KCNQ1_{C214A}$ -injected *X. laevis* oocytes. Oocytes were depolarized for 10 sec to membrane potentials of -60 , -40 , -20 and 0 mV from a holding potential of -80 mV (control: solid line, filled squares; 0.1 mM TMS: dotted line, filled circles.) (A–C) Upper panels. The current size was determined at the end of a 10-sec depolarizing step to the respective clamp voltage. At this time point, TMS increased the $KCNQ1_{wt}$ and $KCNQ1_{C331A}$

currents at -40 mV but decreased these currents at 0 mV. The I/V curve of $KCNQ1_{C214A}$ currents was not altered by TMS. (A–C) Lower panels. I/V relationships of currents determined after 0.2 sec of depolarization to the respective clamp voltage. The increase in $KCNQ1_{wt}$ and $KCNQ1_{C331A}$ current by TMS indicated an acceleration of the early phase of current activation, which is absent for $KCNQ1_{C214A}$ currents.

versible increase in $[Ca^{2+}]_i$. This Ca^{2+} increase showed characteristics of a capacitive Ca^{2+} influx stimulated by store depletion [20]. The patch-clamp experiments performed at “low Ca^{2+} ” suggest that the delayed current increase of I_K is not solely due to the delayed rise in $[Ca^{2+}]_i$ since the current increase could also be observed under these “low Ca^{2+} ” conditions. In addition, the delayed current increase of I_K was reversible upon washout of TMS while the increase in $[Ca^{2+}]_i$ was not. We did not try to further identify the mechanism by which TMS leads to the delayed current increase. However, this effect likely depends on the expression system used, since even after prolonged exposure TMS did not increase I_K in *X. laevis* oocytes. This idea is supported by the finding that different effects of TMS on cytosolic Ca^{2+} and pH have been shown in different cell types [1, 8, 10, 14, 22, 29].

Although these first experiments provided evidence that the effects of TMS are not caused by changes in pH_i or $[Ca^{2+}]_i$ they left the question unanswered whether the initial, divergent effects on I_K and I_{Ks} are due to a direct sulfhydryl oxidation of KCNQ1. The only way to address this question directly was to mutate the cysteine residues at position 214 and 331 to alanines. We did not mutate C136 for three reasons. First, we considered this cysteine an unlikely candidate for the TMS effect because it is located in the first transmembrane-spanning domain S1 and therefore less likely involved in gating mechanisms. Second, C136 is more distant from the extracellular space than C214 or C331 and for this reason is probably less accessible. Third, the performed experiments revealed that TMS did not affect currents of $KCNQ1_{C214A}$ channels, while it affected $KCNQ1_{C331A}$ and $KCNQ1_{wt}$ in a virtually identical

Table 1. Activation time constants derived from fits of a double-exponential function (Eq. 1)

	-40 mV						0 mV									
	τ_1 [sec]		$\Delta\tau_1$ [sec]		τ_2 [sec]		$\Delta\tau_2$ [sec]		τ_1 [sec]		$\Delta\tau_1$ [sec]		τ_2 [sec]		$\Delta\tau_2$ [sec]	
	Con	TMS	Con	TMS	Con	TMS	Con	TMS	Con	TMS	Con	TMS	Con	TMS	Con	TMS
I_{Kwt}	0.4 ± 0.1	0.7 ± 0.1	0.2 ± 0.1*	0.3 ± 0.5	3.7 ± 0.5	5.1 ± 0.5	1.4 ± 0.3*	0.4 ± 0.0	0.3 ± 0.0	-0.1 ± 0.0*	2.9 ± 0.1	2.5 ± 0.2	-0.5 ± 0.1*			
I_{KC331A}	1.0 ± 0.3	1.8 ± 0.4	0.8 ± 0.2*	7.0 ± 1.7	5.1 ± 1.1	7.0 ± 1.7	1.9 ± 0.7*	0.4 ± 0.1	0.3 ± 0.0	-0.1 ± 0.0*	2.4 ± 0.3	2.1 ± 0.3	-0.3 ± 0.0*			
I_{KC214A}	0.6 ± 0.1	0.6 ± 0.1	0.1 ± 0.1	6.1 ± 0.6	5.7 ± 0.5	6.1 ± 0.6	0.4 ± 0.2	0.4 ± 0.0	0.4 ± 0.0	0.0 ± 0.0	3.3 ± 0.3	3.2 ± 0.3	-0.1 ± 0.1			

*Indicates statistical significance ($p < 0.05$). Note that in case of I_{Kwt} and I_{KC331A} , 0.1 mM TMS increased τ_1 and τ_2 at -40 mV, but decreased τ_1 and τ_2 at 0 mV. TMS did not change time constants of I_{KC214A} .

way. Therefore, the effects of TMS on KCNQ1 currents in oocytes could be linked to an oxidation of C214. In the first set of experiments, TMS induced a current decrease in $I_{KCNQ1_{wt}}$ and $I_{KCNQ1_{C331A}}$ but not in $I_{KCNQ1_{C214A}}$ injected oocytes. This finding provides first evidence that TMS interacts with C214. The fact that DTE reversed the TMS-induced current decrease does not indicate that TMS interacts with one of the cysteine residues of KCNQ1. DTE could also reduce a different protein that regulates KCNQ1 channel activity. However, the finding that DTE only reversed the TMS effects on I_{Kwt} and I_{KC331A} but does not affect I_{KC214A} after the exposure to TMS speaks in favor for the interaction of TMS with C214.

This is also supported by the effect of TMS on gating properties of KCNQ1 currents. Deactivation time courses were decelerated in $I_{KCNQ1_{wt}}$ and $I_{KCNQ1_{C331A}}$ but not in $I_{KCNQ1_{C214A}}$ injected oocytes. The effect of TMS on activation kinetics of KCNQ1 currents was more complex, but again absent in I_{KC214A} . The rapid saturation of outward current has been attributed to the activation and delayed inactivation of homomeric KCNQ1 channels [19]. As suggested by Figs. 5–7, TMS might facilitate both, activation and inactivation of I_{Kwt} and I_{KC331A} . At a depolarizing step to -40 mV, at which delayed inactivation is largely absent [30], TMS increased these activation currents throughout the time course. At a depolarizing step to 0 mV, at which inactivation starts with a delay of some 100–200 msec [19, 30], TMS increased initial I_{Kwt} and I_{KC331A} , but decreased these currents at a later time point (Figs. 5–7). Activation currents of $I_{KCNQ1_{C214A}}$ channels were not affected by TMS.

In summary, our results strongly suggest that TMS interacts with the cysteine residues 214 in the S3 domain and modifies deactivation and activation kinetics of homomeric KCNQ1 channels. Since TMS was originally reported to increase the current amplitude of I_{Ks} and to accelerate its activation kinetics [33], we investigated the effect of TMS on I_{Ks} of KCNE1-, $I_{KCNQ1_{wt}/KCNE1}$ -, $I_{KCNQ1_{C331A}/KCNE1}$ - and $I_{KCNQ1_{C214A}/KCNE1}$ -injected oocytes. In contrast to currents of homomeric channels, TMS increased currents throughout the entire voltage range tested. The current increase of $I_{KCNQ1_{C214A}/KCNE1}$ -injected oocytes at 0 mV, though, was smaller than that of $I_{KCNQ1_{wt}/KCNE1}$ - and $I_{KCNQ1_{C331A}/KCNE1}$ -injected oocytes. In contrast to the effect of TMS on homomeric $I_{KCNQ1_{C214A}}$ channels TMS still induced a small but significant increase in current of heteromeric $I_{KCNQ1_{C214A}/KCNE1}$ channels. Since *X. laevis* oocytes endogenously express xKCNQ1, it is expected that in $I_{KCNQ1_{C214A}/KCNE1}$ -injected oocytes xKCNQ1/KCNE1 channels and “species-heteromeric” channels, consisting of xKCNQ1,

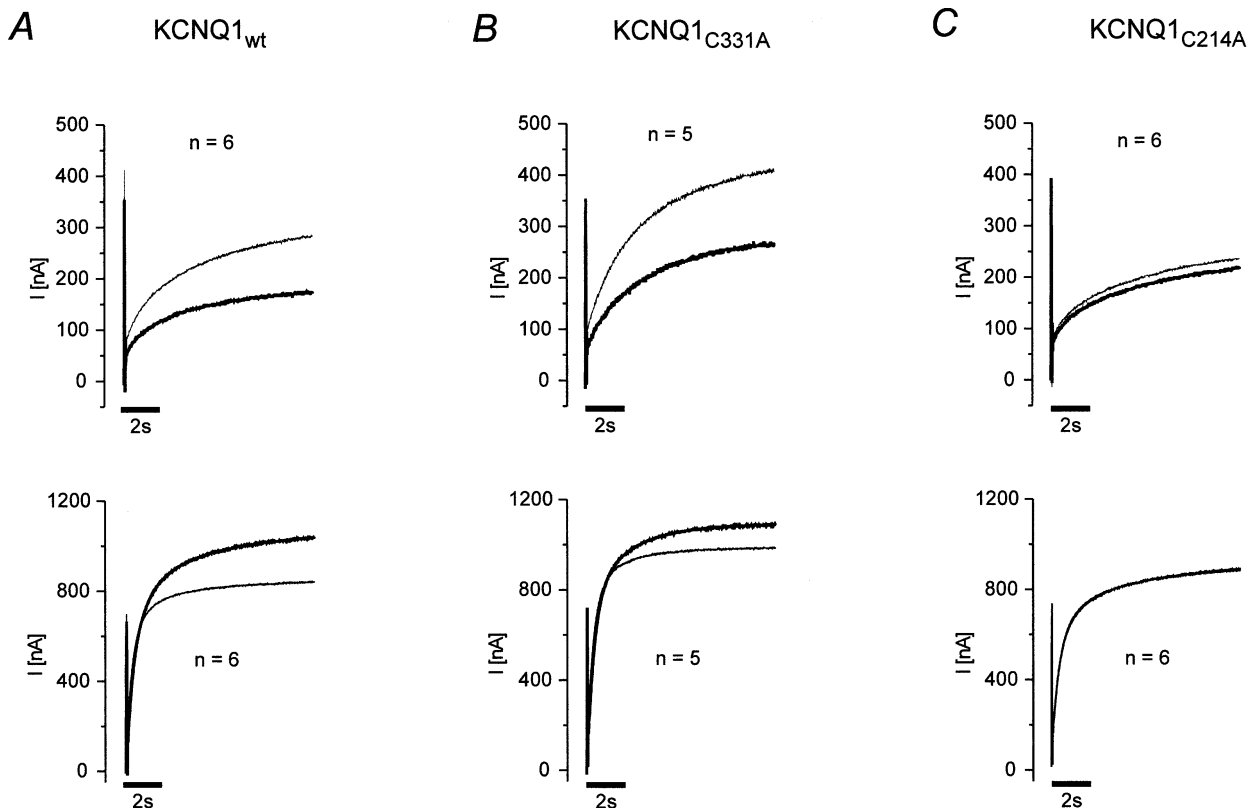


Fig. 7. (A–C) Activation kinetics of mean KCNQ1 currents at -40 mV (*upper panels*) and at 0 mV (*lower panels*). The oocytes were depolarized for 10 sec to the respective voltage from a holding potential of -80 mV. Control: *solid line*; 0.1 mM TMS: *thin line*.

Note that at -40 mV, TMS increased KCNQ1_{wt} and KCNQ1_{C331A} currents during the initial and the later phase of activation. At 0 mV, TMS initially increased and decreased these two currents during the later phase of activation.

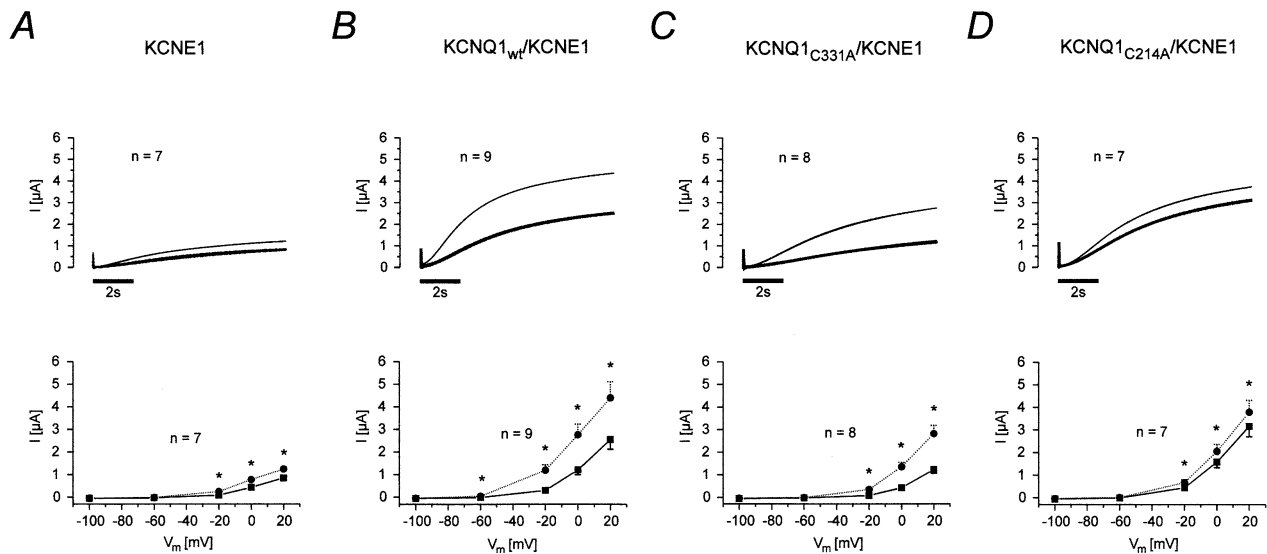


Fig. 8. Activation kinetics and I/V relationships of KCNQ1/KCNE1 (I_{K_s}) channels (A–D) The type of cRNA injected is indicated at the top of figures. *Upper panels*: current activation kinetics at $+20$ mV. Control: *solid line*; 0.1 mM TMS: *thin line*. *Lower panels*: I/V relationships of currents. Oocytes were held at a clamp voltage of -100 mV and depolarized for 10 sec to a membrane voltage of -60 , -20 , 0 and $+20$ mV. Control: *solid lines*, *filled squares*; 0.1 mM TMS: *dotted line*, *filled circles*. (A) In KCNE1-injected oocytes, KCNE1 coassembled with the endogenous

xKCNQ1 to form xKCNQ1/KCNE1 currents, which were slightly increased by TMS. (D) In a similar fashion, KCNQ1_{C214A}/KCNE1-injected oocytes showed a poor augmentation by TMS. The increase is probably due to xKCNQ1/KCNE1 currents, which still can form in spite of coinjection with KCNQ1_{C214A}. (B,C) The currents of KCNQ1_{wt}/KCNE1- and KCNQ1_{C331A}/KCNE1-injected oocytes were significantly more increased at 0 and $+20$ mV than currents of KCNE1- or KCNQ1_{C214A}/KCNE1-injected oocytes.

KCNQ1_{C214A} and KCNE1 subunits, form I_{Ks} . As shown in the original report and in the control group of our study, the I_{Ks} current of KCNE1-injected oocytes could be increased by TMS. This increase of xKCNQ1/KCNE1 channels was not statistically different from the increase of KCNQ1_{C214A}/KCNE1 channels. In fact, the cysteine residue in S3 is conserved in xKCNQ1 and very likely interacts with the sulfhydryl reagent TMS resulting in the current increase of heteromeric xKCNQ1/KCNE1 channels.

How can the presented results be incorporated into the current knowledge of the structure-function relationship of voltage-gated K^+ channels? Voltage-gated K^+ channels are thought to consist of 4 identical subunits [12]. Each of these subunits has six transmembrane spanning segments (S1–S6) and a hairpin loop between S5 and S6 that determines the selectivity of the channel. The positively charged segment S4 very likely plays the key role in voltage sensing [13, 17] and shifts towards the extracellular space during activation [11, 13]. S4 has been proposed to be located in the center of each subunit, surrounded by the other segments and the P-loop. S1–S3 and S5 are thought to form the outer shell facing the membrane lipid bilayer, while the P-loop and S6 are thought to form the inner shell and part of the pore [6]. From this model it seems reasonable to assume that because of its proximity to S4, S3 might be involved in channel gating as well. In fact, there is evidence that in voltage-gated K^+ channels S3 and S2 are involved in channel gating [18, 26]. It is interesting to note, however, that in our study, the interaction of TMS with C214 did not only seem to change activation but also inactivation. This is of special interest since in spite of many similarities in the structure-function relationship between the *Shaker*- and the KCNQ-family, KCNQ1 does not inactivate by a typical N- or C-type mechanism [19, 30]. The presented results indicate that in KCNQ1 channels, S3 might be one of the determinants in ion channel inactivation. It is still not understood how KCNE1 hinders inactivation in heteromeric KCNQ1/KCNE1 channels. Based on two-hybrid and affinity chromatography assays it has been proposed that the cytoplasmatic C-terminus of KCNE1 interacts with the pore region leading to an increased open probability [21]. Electrophysiological analysis of KCNE1 mutants provided evidence that the transmembrane segment of KCNE1 forms part of the pore [27]. Both models are consistent with a role of S3 in channel gating, since in both models KCNE1 would be able to override the mechanism by which S3 induces inactivation in homomeric KCNQ1 channels. It is interesting though, that S3 would nonetheless be able to determine the activation of the heteromeric channel.

In summary we conclude that the effects of TMS on the gating properties of homomeric

KCNQ1 and heteromeric KCNQ1/KCNE1 channels can be explained by an interaction with the cysteine residue C₂₁₄ in the S3 segment of KCNQ1. This suggests that not only the inner shell, but also the outer shell of the KCNQ1 channel is important for the gating behavior of voltage-dependent K^+ channels. It is exciting to speculate that this channel region might be involved in channel activation and inactivation.

The authors thank Dr. S.J. Kim for his outstanding support and helpful discussions and G. Kummer, H. Schauer, A. Bausch and Dr. U. Fröbe for their excellent assistance with this work. We gratefully acknowledge the help from Aventis Pharma, Frankfurt, Germany. This work was supported by Deutsche Forschungsgemeinschaft (DFG Gr 480/11-3).

References

1. Bootman, M.D., Taylor, C.W., Berridge, M.J. 1992. The thiol reagent, thimerosal, evokes Ca^{2+} spikes in HeLa cells by sensitizing the inositol 1,4,5-trisphosphate receptor. *J. Biol. Chem.* **267**:25113–25119
2. Busch, A.E., Busch, G.L., Ford, E., Suessbrich, H., Lang, H.J., Greger, R., Kunzelmann, K., Attali, B., Stühmer, W. 1997. The role of the IsK protein in the specific pharmacological properties of the IKs channel complex. *Br. J. Pharm.* **122**:187–189
3. Busch, A.E., Lang, F. 1993. Effects of $[Ca^{2+}]_i$ and temperature on minK channels expressed in *Xenopus* oocytes. *FEBS Letters* **334**:221–224
4. Chiamvimonvat, N., O'Rourke, B., Kamp, T.J., Kallen, R.G., Hofmann, F., Flockerzi, V., Marban, E. 1995. Functional consequences of sulfhydryl modification in the pore-forming subunits of cardiovascular Ca^{2+} and Na^{2+} channels. *Circ. Res.* **76**:325–334
5. Coetzee, W.A., Nakamura, T.Y., Faivre, J.F. 1995. Effects of thiol-modifying agents on K_{ATP} channels in guinea pig ventricular cells. *Am. J. Physiol* **269**:H1625–H1633
6. Durell, S.R., Hao, Y., Guy, H.R. 1998. Structural models of the transmembrane region of voltage-gated and other K^+ channels in open, closed, and inactivated conformations. *J. Struct. Biol.* **121**:263–284
7. Grynkiewicz, G., Poenie, M., Tsien, R.Y. 1985. A new generation of Ca^{2+} indicators with greatly improved fluorescence properties. *J. Biol. Chem.* **260**:3440–3450
8. Gukovskaya, A.S., Trepakova, E.S., Zinchenko, V.P., Korystov, Y.N., Bezuglov, V.V. 1992. Effect of the sulfhydryl reagent thimerosal on cytosolic free Ca^{2+} and membrane potential of thymocytes. *Biochim. Biophys. Acta* **1111**:65–74
9. Kerst, G., Fischer, K.G., Normann, C., Kramer, A., Leipziger, J., Greger, R. 1995. Ca^{2+} influx induced by store release and cytosolic Ca^{2+} chelation in HT₂₉ colonic carcinoma cells. *Pflügers Arch.* **430**:653–665
10. Kimura, M., Nakamura, K., Fenton, J.W., Andersen, T.T., Reeves, J.P., Aviv, A. 1994. Role of external Na^+ and cytosolic pH in agonist-evoked cytosolic Ca^{2+} response in human platelets. *Am. J. Physiol.* **267**:C1543–C1552
11. Larsson, H.P., Baker, O.S., Dhillon, D.S., Isacoff, E.Y. 1996. Transmembrane movement of the *Shaker* K^+ channel S4. *Neuron* **16**:387–397
12. MacKinnon, R. 1991. Determination of the subunit stoichiometry of a voltage-activated potassium channel. *Nature* **350**:232–235

13. Mannuzzo, L.M., Moronne, M.M., Isacoff, E.Y. 1996. Direct physical measure of conformational rearrangement underlying potassium channel gating. *Science* **271**:213–216
14. Martin, F., Gualberto, A., Sobrino, F., Pintado, E. 1991. Thimerosal induces calcium mobilization, fructose 2,6-bisphosphate synthesis and cytoplasmic alkalinization in rat thymus lymphocytes. *Biochim. Biophys. Acta* **1091**:110–114
15. Nitschke, R., Fröbe, U., Greger, R. 1991. Antidiuretic hormone acts via V_1 receptors on intracellular calcium in isolated perfused rabbit cortical thick ascending limb. *Pflügers Arch.* **417**:622–632
16. Nitschke, R., Riedel, A., Ricken, S., Leipziger, J., Benning, N., Fischer, K., Greger, R. 1996. The effect of intracellular pH on cytosolic Ca^{2+} in HT₂₉ cells. *Pflügers Arch.* **433**:98–108
17. Papazian, D.M., Timpe, L.C., Jan, Y.N., Jan, L.Y. 1991. Alteration of voltage-dependence of *Shaker* potassium channel by mutations in the S4 sequence. *Nature* **349**:305–310
18. Planells-Cases, R., Ferrer-Montiel, A.V., Patten, C.D., Montal, M. 1995. Mutation of conserved negatively charged residues in the S2 and S3 transmembrane segments of a mammalian K^+ channel selectively modulates channel gating. *Proc. Natl. Acad. Sci. USA* **92**:9422–9426
19. Pusch, M., Magrassi, R., Wollnik, B., Conti, F. 1998. Activation and inactivation of homomeric KvLQT1 potassium channels. *Biophys. J.* **75**:785–792
20. Putney, J.W., Bird, G.St.J. 1993. The signal for capacitative calcium entry. *Cell* **75**:199–201
21. Romey, G., Attali, B., Chouabe, C., Abitbol, I., Guillemare, E., Barhanin, J., Lazdunski, M. 1997. Molecular mechanism and functional significance of the MinK control of the KvLQT1 channel activity. *J. Biol. Chem.* **272**:16713–16716
22. Ruddock, N.T., Machaty, Z., Milanick, M., Prather, R.S. 2000. Mechanism of intracellular pH increase during parthenogenetic activation of In vitro matured porcine oocytes. *Biol. Reprod.* **63**:488–492
23. Ruppersberg, J.P., Stocker, M., Pongs, O., Heinemann, S.H., Frank, R., Koenen, M. 1991. Regulation of fast inactivation of cloned mammalian IK(A) channels by cysteine oxidation. *Nature* **352**:711–714
24. Sanguinetti, M.C., Curran, M.E., Zou, A., Shen, J., Spector, P.S., Atkinson, D.L., Keating, M.T. 1996. Coassembly of KvLQT1 and minK (IsK) proteins to form cardiac I_{Ks} potassium channel. *Nature* **384**:80–83
25. Schulte, U., Hahn, H., Wiesinger, H., Ruppersberg, J.P., Fakler, B. 1998. pH-dependent gating of ROMK ($K_{ir1.1}$) channels involves conformational changes in both N and C termini. *J. Biol. Chem.* **273**:34575–34579
26. Seoh, S.A., Sigg, D., Papazian, D.M., Bezanilla, F. 1996. Voltage-sensing residues in the S2 and S4 segments of the *Shaker* K^+ channel. *Neuron* **16**:1159–1167
27. Tai, K.K., Goldstein, S.A. 1998. The conduction pore of a cardiac potassium channel. *Nature* **391**:605–608
28. Thiele, I.E., Hug, M.J., Hübner, M., Greger, R. 1998. Expression of cystic fibrosis transmembrane conductance regulator alters the responses to hypotonic cell swelling and ATP of Chinese hamster ovary cells. *Cell. Physiol. Bioch.* **8**:61–74
29. Thorn, P., Brady, P., Llopis, J., Gallacher, D.V., Petersen, O.H. 1992. Cytosolic Ca^{2+} spikes evoked by the thiol reagent thimerosal in both intact and internally perfused single pancreatic acinar cells. *Pflügers Arch.* **422**:173–178
30. Tristani-Firouzi, M., Sanguinetti, M.C. 1998. Voltage-dependent inactivation of the human K^+ channel KvLQT1 is eliminated by association with minimal K^+ channel (minK) subunits. *J. Physiol.* **510**:37–45
31. Unsold, B., Kerst, G., Brousos, H., Hubner, M., Schreiber, R., Nitschke, R., Greger, R., Bleich, M. 2000. KCNE1 reverses the response of the human K^+ channel KCNQ1 to cytosolic pH changes and alters its pharmacology and sensitivity to temperature. *Pflügers Arch.* **441**:368–378
32. Yang, W.P., Levesque, P.C., Little, W.A., Conder, M.L., Shalaby, F.Y., Blam, M.A. 1997. KvLQT1, a voltage-gated potassium channel responsible for human cardiac arrhythmias. *Proc. Natl. Acad. Sci. USA* **94**:4017–4021
33. Yao, J.A., Jiang, M., Tseng, G.N. 1997. Mechanism of enhancement of slow delayed rectifier current by extracellular sulfhydryl modification. *Am. J. Physiol.* **273**:H208–H219